คำแนะนำในการเตรียมการทดลอง

PROCEDURE IN A LABORATORY AND THE LABORATORY NOTEBOOK

Naturally, the actual procedure to be followed during the data-taking part of the experiment varies greatly depending on the nature of the experiment. However, certain general truths obtain in all situations. The most important requirement of the actual laboratory phase of the work is a thorough understanding of the goals and plan of the experiment. Preparation cannot be stressed too much as the greatest requirement of a successful experiment.

The ability to think on one's feet during an experiment is one of the talents that an instructional laboratory program is designed to foster. This ability, however, is meaningless unless the scientist (or student-scientist) has entered the laboratory with a clear idea of what he intends to do. The more difficulties that the scientist can anticipate in advance, the more likely is the success of the whole venture. Orderliness both in habits of thought about the experimen: and in the actual performance of the physical manipulations required to make the observations and record the data are universal attributes of the professional experimenter.

The Laboratory Notebook

The recording of the data of the experiment is no less important than the setting up of the experimental equipment and the manipulations with it. One must always keep in mind that the scientist may often remember no more about the data-taking stage than is written in his notebook. All relcvani information must be written down in easily intelligible form.

PERMANENCE AND COMPLETENESS

It is strongly recommended that the pages of the laboratory notebook be numbered and that they be bound so that none may be removed. The date, time, and name of the person taking data should be written as soon as the experimental work is commenced. Diagrams of the equipment, circuits, and mechanical structures must be noted. If particular instruments are used, their identifying numbers should be recorded acd any peculiarities of operation remarked. If calibration procedures are required or if reliable calibrations exist, they should be recorded in the laboratory notebook or their location noted. Any information that conceivably could help in reconstructing what one has done or what happended in the laboratory should be recorded. An almost universal experience of experimental scientists is that even apparently irrelevant pieces of information have helped at one time or

another in recovering data or correcting mistakes. If one is not sure that a temperature correction need be made, he should record the ambient temperature anyway. The sparks being generated by a machine across the corridor may not affect the experiment, but the situation should be noted in any case. Observations made can be ignored and data can be discarded, but there is no solution if a vital fact has not been recorded.

CORRECTIONS

It is also strongly recommended that the entries in the laboratory notebook be made in ink and that erasures not be made. If it is believed that incorrect entries have been made, the errors should be neatly crossed out with a fine line and corrections entered. If one has occasion to make entries on previous pages that were initially written at an earlier time, the date and time of the added entries should be noted as well as the name of the person making the additions. Mistakes are always a possibility. Not infrequently the mistake was in making the addition, and by avoiding erasures one has preserved the original, sometimes correct, entries. Often collaborating scientists may disagree about the validity of an entry. By signing and dating corrections, additions, or deletions (crossing out), the ultimate decision may be postponed until a thorough discussion is possible among the investigators concerned.

SUMMARIES

Summaries and preliminary data reductions should be made as soon as possible during the course of the data taking. This serves to uncover mistakes and generally helps to determine whether or not one is on the right track. If one discovers errors in procedure or malfunctions of equipment while yet in the laboratory, the fault is not permanent and may be rectified before leaving the laboratory. Constant checking of what one observes against what one expects is an integral part of the "thinking on one's feet" that is so essential to successful experimental work. Analysis while the situation is still fresh in the experimenter's mind is usually more fruitful of uncovering errors and deficiencies. Data grow stale and an experienced scientist often regards with a jaundiced eye an experiment reported too long after the data were actually taken. A successful experiment requires thorough understanding and control of the experimental situation. As the scientist's recollection of what happened dims with the passing of time, so do his chances of completely reconstructing and understanding what was happening.

ตัวอย่างการเขียนรายงานทางวิทยาศาสตร์

ตัวอย่างที่ 1 *Am. J. Phys.* 50(1), Jan. 1982 p 38-41.

Advanced undergraduate laboratory experiment in inelastic electron tunneling spectroscopy

H.W. White and R.J. Graves

Physics Department, University of Missouri-Columbia, Columbia, Missouri 65211.

(Received 20 November 1980; accepted for publication 18 February 1981)

An advanced undergraduate laboratory experiment in inelastic electron tunneling spectroscopy is described. The project was done by junior- and senior-level students. Tunnel junctions were fabricated, the tunneling spectra of several molecules adsorbed on the surface of aluminum oxide measured, and mode assignments made for several of the prominent peaks in the spectra using results obtained from optical studies.

I. INTRODUCTION

Inelastic electron tunneling spectroscopy (IETS) is a new technique that provides a versatile and sensitive method for measuring the vibrational spectrum of a molecular species adsorbed on the surface of a metal oxide. This article describes an advanced undergraduate laboratory experiment in IETS. Tunnel junctions doped with one of several molecular species were prepared in a high-vacuum evaporator and spectra obtained on those with desirable electrical characteristics. Several of the vibrational modes of the adsorbed species were identified using literature values for characteristic mode frequencies and comparison with deuterated species.

This laboratory experiment was designed to acquaint students with a number of useful experimental techniques including use of high-vacuum systems, vapor deposition of metals, handling of cryogenic liquids, modulation spectroscopy, and signal averaging techniques. It is one of several experiments in a new laboratory course required of all of our physics majors. Each student selects four or five experiments from those available which include x-ray scattering, NMR, ESR, Raman scattering, low-temperature thermometry, optical absorption, and IETS. During each experiment, the students (usually four) work very closely with an instructor who has been or is currently engaged in research in the area. Some of the experiments are done in the respective research laboratories.

This article describes the experiment performed by the students. It provides information on experimental procedures and equipment, including circuit diagrams, so that it can serve as a guide for students who wish to do an experiment in IETS.

The general features of IETS are presented in Sec. II. Section III, on experimental procedure, contains more detailed information on how the tunnel junctions were fabricated,

checked, and measured. The spectrometer circuit with grounding and shielding is provided. The design is modular to facilitate construction and substitution of available equipment.

Additional information on IETS can be obtained from several articles including those of Simonsen, *et al*.[1] and from a review of IETS by Hansma[2]

II. GENERAL FEATURES OF IETS

IETS involves the measurement of the electrical current I associated with electrons that tunnel through an oxide film having an adsorbed molecular layer on its surface. The electrons that inelastically tunnel through the oxide excite the characteristic vibrations of the adsorbed molecules. Graphs of the second derivative d^2I/dV^2 versus the bias voltage V display large peaks centered at the voltage $V_m = h\nu_m/e$, where h is Planck's constant, e is the electronic charge, and ν_m is molecular vibrational frequency. These graphs show peaks that can be associated with the presence of both infrared and Raman-like modes. The spectra can be used to identify molecular species on the oxide layer, estimate molecular orientation, and detect chemisorption bonding to the oxide layer. The molecular species to be studied is placed in contact with an oxidized metal film. Another metallic film (usually lead) is evaporated over the "doped" oxide to form a metal-insulator-metal tunnel junction, as shown in Fig. 1. The junction is then cooled to liquid helium temperatures and the spectrum measured.

If a variable bias is applied acorss the junction terminals and the current is measured, only a small current of the order of milliamperes will flow across the junction since the oxide layer is an excellent insulator. This current is due to electrons that tunnel (in the quantum-mechanical sense) through the insulating oxide barrier. This tunneling current has contributions from both elastic and inelastic processes. Figure 2(a) illustrates the elastic

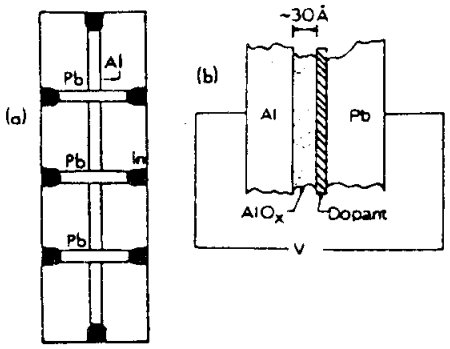

Fig. 1. Representation of a substrate showing three junctions is shown in (a). The long, vertical strip represents the aluminum electrode and the three short, horizontal strips, the lead electrodes. The black areas at the ends of the evaporated metal strips are indium solder pads. A schematic of the cross section of an aluminum-aluminum-oxide-dopant-lead tunnel junction showing the application of a bias voltage V is shown in (b).

tunneling process in which an electron tunnels through the oxide barrier from an occupied state below the Fermi level in the aluminum to an unoccupied electron state above the Fermi level of the lead film. Electrons that tunnel without loss of energy contribute to the elastic tunneling current. Figure 2(b) illustrates an inelastic tunneling process. In this case the tunneling electron interacts with a molecule adsorbed on the oxide and excites one of the characterstic vibrational modes of the molecule. For a molecular vibrational frequency ν_m the energy lost by the tunneling electron will be $h\nu_m$. It is evident from the diagram that the threshold bias for such an inelastic tunneling event is $eV_{threshold} = h\nu_m$. There is a different threshold voltage for each vibrational mode of the molecules on the oxide. At a threshold voltage there is an abrupt change in the slope of the current-voltage characteristic of the tunnel junction since a new channel for the inelastic tunneling process is then available. This change is illustrated in Fig. 2(c). Electronic modulation methods are used to record the junction conductance $G = dI/dV$ and the second derivative d^2I/dV^2 in order to enhance the detection of this effect. The opening up of a new channel changes the conductance by a percent or so as illustrated in Fig. 2(d). The effect in d^2I/dV^2 is very large as shown in Fig. 2(e) since the only sharp structure in the conductance is due to inelastic tunneling.

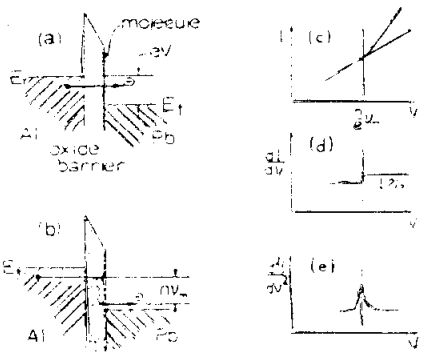

Fig. 2. Diagrams of (a) the elastic and (b) inelastic tunneling processes occuring between the two junction electrodes. The current-voltage characteristics near $eV = h\nu_m$ resulting from inelastic tunneling are shown in (c), (d), and (e).

III. EXPERIMENTAL PROCEDURE

This section describes the experimental equipment and techniques employed by the students. It is divided into discussions of junction preparation and measurement of spectra.

A. Junction preparation

A schematic of the vacuum chamber is shown in Fig. 3. Two tungsten dimple boats, $10 \times 100 \times 0.012$ mm, were loaded with charges of pure aluminum and lead, respectively. A clean 25×75-mm microscope slide was placed on a mask made from 0.012-mm brass shim

stock, which had an aperture I x25 mm along its center. The system was closed, and a IS-min glow discharge at 0.03 A in 0.08 Torr oxygen (99.9% pure) was used to scrub the chamber. The negative electrode for the glow discharge was a piece of aluminutn sheet of about 100 cm* while the base of the vacuum chamber acted as the positive electrode. The chamber was then evacuated to about 10^{-6} Torr. and an aluminum electrode of about 1000 Å thickness was evaporated onto the glass substrate. The evaporation proceeded by melting small pieces of 99.999% aluminum in a tungsten dimple boat,[3] opening the shutter, and observing along the line of sight shown in Fig. 3 When the deposition was opaque (about 30 sec of evaporation), the shutter was rotated to the closed position. The current through the boat was then decreased slowly to avoid cracking the tungsten.

The freshly evaporated aluminum strips were then oxidized in a glow discharge of 0.8 Torr oxygen at 0.03 A for about 15 min. This exposure was sufficient to grow an oxide layer 15-20 Å in thickness. These substrates were then removed from the chamber and doped with the molecular species of interest outside the vacuum chamber. Junctions doped with formamide $HCONH_2$ will be discussed in this article. Thiourea has also been used. The substrates were then quickly returned to the vacuum chamber, placed on another brass electrode mask, and lead electrodes evaporated in a manner similar to that used for aluminum.

An oil diffusion-mechanical pumping system was used to achieve the desired chamber pressures. Cold traps were placed in the mechanical and diffusion pump lines leading to the vacuum chamber to avoid contamination from forepump oil. As an added precaution the chamber was not roughed below 0.050 Torr with the mechanical pump.

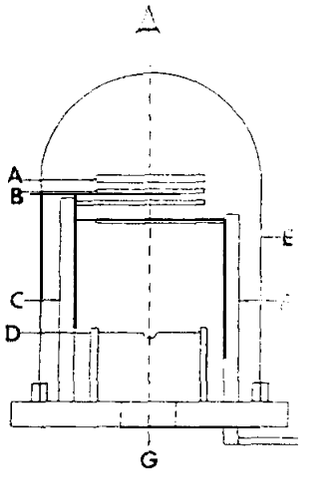

Fig. 3. Schematic of the evaporation chamber showing relative positions of (a) the microscope slide-substrate, (b) the evaporation mask, (c) the substrate holder assembly, (d) the tungsten dimple boats, (e) the bell jar, (f) the rotating shutter assembly, and (g) the line of sight for deposition thickness monitoring. The vertical distance between the evaporation boats and the substrates is about 30 cm.

The junctions were removed from the bell jar and indium contacts were applied to the ends of the junction metal strips, as illustrated in Fig. 1, using a low-power soldering iron. The junctions's resistances were then checked using low power to avoid damage to the junctions. In this experiment an ac signal generator was connected in series with the junction and a variable resistance box. The junction resistance could then be determined by adjustment of the variable resistance until equal voltages were obtained across each, as indicated on an x-y scope. Junctions that had nominal resistance values in the range 50-5000 Ω were stored in a dessicator until ready for measurement.

B. Measurement of spectra

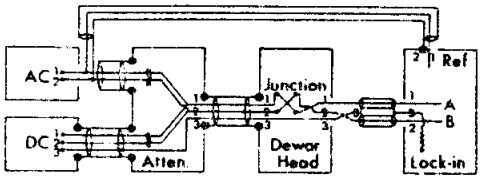

Fig. 4. Schematic of spectrometer circuit showing the grounding and shielding arrangement. Line 3 in the dc supply can be grounded to the shield by a contact switch. The output of the lock-in is proportional to dV/dI or d^2V/DI^2 when operated in the first or second harmonic mode, respectively.

Figure 4 is a schematic of a grounding and shielding arrangement for measuring dV/dI. The details of the attenuator box are shown in Fig. 5. Coaxial cables are used extensively. The dc bias voltage V developed across the junction can be obtained by employing tees between the dewar head and lock-in amplifier; Spectra of d^2V/dI^2 vs V can be obtained by the addition of an ac amplifier and filter (twin-tee notch at f_0 or pass at $2f_0$) just before the input to the lock-in, which is operated in the second harmonic mode.

A junction with an appropriate resistance value was connected to the dewar head probe and immersed in liquid helium. The dc sweep supply was set to the value at the high end of the sweep (e.g., 10V). The resistance R_1 (Fig. 5) was then adjusted to obtain a bias voltage of 500 mV across the junction. The bias voltage was then reduced to a value associated with the highest peak expected in the spectrum (e.g., C – H stretch near 355 meV) and the "phase" adjusted on the lock-in to show the smallest "out-of-phase" component. The full-scale sensitivity of the lock-in and the magnitude of the modulation signal were varied (R_2, R_3) until a slow sweep of the bias voltage from 30 to 500 mV gave a good spectrum with nearly full-scale deflection at the highest peak. Typical values used when measuring d^2V/dI^2vs V were as follows:

ac modulation	2 – 4 mV (rms)
dc sweep across junction	30 – 500 mev

Sweep speed	0.5 mV/sec
ac amplifier gain	×20
Lock-in sensitivity	0.1 mV f.s.
Lock-in time constant	1 sec.

Spectra were presented to an electronic signal averager in this experiment and then recorded on an x-y recorder. The dc sweep was also supplied by the signal averager. A battery with a ten-turn potentiometer can also be used effectively. When a substrate was removed from the liquid helium bath, a warm air blower was used to warm the substrate to room temperature quickly (without overheating it) and to evaporate all the water that formed on the junction (water will oxidize the lead electrodes rendering a junction useless for future measurements).

The cryostat used to cool the junctions was a rather simple dewar system. A substrate was fastened to a long probe with low thermal conductivity using small copper alligator clips to contact the indium pads and was lowered into the liquid helium bath. The input leads were a twisted pair, as were the two signal leads.

It was earlier noted that the resistance values of junctions at room temperature should be in the range 50-5000 Ω. Good quality junctions should show a small increase in resistance when taken from 300 to 4.2k. A decrease indicates the presence of metallic shorts. These junctions should not be used. Junctions with resistances higher than 5000 Ω are generally noisy. Thin spots in the oxide layer will cause the current to pass through only a small region of the surface so that spectra from such junctions will show little detail. Junctions stored in clean, dry dessicators will often give good spectra as long as three to four months later depending on the dopant molecule used.

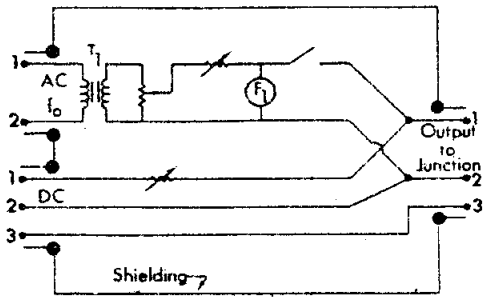

Fig. 5. Schematic of the attenuator box circuit. T_1 is a UTC-LS140 isolation transformer. F_1 is a twin-tee 2000-Hz notch filter (f_0 is 1000 Hz). R_1 is six-decade series with 1000 kΩ per step on the highest resistance decades. R_2 is a three decade series with 1000 kΩ per step on the highest resistance decade. R_3 is a 20-kΩ ten-turn potentiometer.

IV. ANALYSIS OF DATA AND RESULTS

Representative spectra obtained by the students for formamide $HCONH_2$ and two deuteroderivatives $DCONH_2$ and $HCOND_2$ are shown in Fig. 6. After obtaining the spectra, the students assigned vibrational modes to the peaks using vibrational frequencies from texts containing infrared and Raman vibrational mode assignments. Some assistance from the instructor was usually necessary in making assignments. The vibrational modes of a tunneling spectrum are generally assigned by comparison with available infrared and Raman data since both types of vibrations will be present in tunneling spectra. Tunneling peak frequencies, however, will often be found at frequencies a few wave numbers lower than their optical counterparts due to effects of the lead overlayer. It should also be noted that peaks associated with vibrational modes of deuterated bonds will be at frequencies lower than their nondeuterated mode frequencies by a factor of approximately $2^{-1/2}$. A useful conversion factor is 8.0625 cm^{-1} = 1 meV. Some of the spectral features are discussed below.

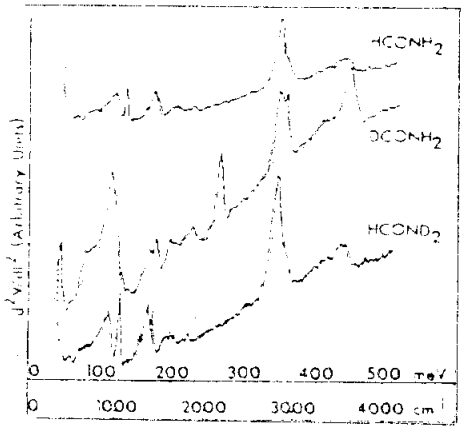

Fig. 6. IETS spectra obtained by students from aluminum-aluminum oxide-lead tunnel junctions doped with formamide $HCONH_2$, and the deuteroderivatives $DCONH_2$ and $HCOND_2$.

Each of the spectra for $HCONH_2$, $DCONH_2$, and $HCOND_2$ showed a peak near 300 cm^{-1} that could be associated with an aluminum metal phonon in the electrode. Other phonons at lower frequencies give rise to very large peaks that dominate the spectral features to the extent that molecular vibrational modes cannot be observed easily. Prominent peaks that occur near 930 cm^{-1} are due to C – H out-of-plane deformation and C – O stretch modes. Peaks assigned as C – H stretch modes appear in all three spectra near 2900 cm^{-1}. Some of these C – H contributions are undoubtedly due to surface contamination acquired during junction fabrication. The peak near 2150 cm^{-1} in the $DCONH_2$ is clearly a C – D stretch since it would be expected to appear for this deuterated form and since its location is approximately $2^{-1/2}$ of the C – H stretch values. the $DCONH_2$ spectrum also shows a broad peak near 3300 cm^{-1} that corresponds to N – H stretch frequencies. All three show O – H stretch frequencies near 3600 cm^{-1}.

V. SUMMARY

An advanced undergraduate laboratory experiment in inelastic electron tunneling spectroscopy has been described. The experiment provides challenging exposure to several experimental techniques that include depositing thin metal films in high vacuum, handling cyrogenic liquids, and operating a low-level ac modulation spectrometer. The response of the students to the experiment has consistently been very positive. This experiment will continue to be offered in our advanced laboratory course.

---

[1]M.G.Simonsen, R.V. Coleman, and P.K. Hansma, *J. Chem Phys.* 61 3789(1974).

[2]P.K. Hansma, *Phys. Rep.* C 30, 145(1977).

[3]Dimple boats, model S41-.005 W, were obtained from R.D.Mathis Co., 2840 Gundry Ave., Long Beach, CA 90806.

ตัวอย่างที่ 2 Am. J. Phys. 50(2). Feb. 1982, p. 113-119.

Experimental investigation of the transverse vibrational frequency ratio for identical loaded and unloaded rubber strings

M.F. Beatty
Department of Engineering Mechanics, University of Kentucky, Lexington, Kentucky 40506

J.H. Lienhard, V
Department of Mechanical Engineering, University of Kentucky, Lexington, Kentucky 40506

(Received 27 October 1980; accepted for publication 3 April 1981)

The elementary problems of small transverse vibrations of loaded and unloaded strings are briefly reviewed, and an example that shows the effect on the vibrational frequency of the amount of stretch of different kinds of materials is presented. A detailed review of the problem of the transverse vibration of a loaded string when the inertia of string is not neglected is presented, and certain exact and approximate results are examined graphically. A Universal formula for the ratio of the fundamental transverse vibrational frequencies of identical loaded and unloaded strings is derived; and new experimental results describing the response of loaded rubber cords for a wide range of attached loads are compared with the universal formula.

I. INTRODUCTION

Investigation of the problem of the small-amplitude motion of a vibrating string usually is included in a beginning course in mechanical vibrations or acoustics. It is learned, though seldom emphasized, that the transverse vibrational frequency derived is a universal result in the sense that it is independent of the elastic behavior of the material. On the other hand, the manner in which the frequency may vary with the amount of stretch, which all too often and unnecessarily is assumed infinitesimal, will depend on the elastic response of the material. The same may be said of the simpler problem of the small-amplitude vibration of a mass attached to an elastic string. In this case, the influnce of the inertia of the string on the motion of the load is commonly neglected. In fact, this effect is not discussed in most textbooks; consequently, we lose the opportunity for the teacher to explore with the student the degree to which the easy approximate solution is valid and for the student to learn method from the analysis of the problem when the inertia of the string is included. We hope that this didactic note will help to remedy the situation and at the same time provide some fresh thoughts together with some new experimental results related to the transverse vibration of identical loaded and unloaded rubber strings.

With these objectives in mind, we shall review briefly in Sec. II the problems of small transverse vibration of loaded and unloaded strings. We present an illustrative example that reveals an interesting effect on the frequency due to variation in material response for two different materials, a highly elastic rubber cord and a typical metal wire. Then, we turn to a careful review of the transverse vibration of the loaded string in the case when the inertia of the string is included. The first- and second-order fundamental-mode approximations, and the higher-mode and nodal solutions are compared graphically with the exact solution; the results are interpreted physically and the extent to which the approximate solutions are meaningful is discussed. It is shown that regardless of the amount of stretch of the string and the nature of its material the ratio of the fundamental transverse vibrational frequencies of identical loaded and unloaded strings is a constant that depends only on the ratio of their masses, a simple result that seems to have passed unnoticed in the usual sources. We also show easily that the frequency of vibration of the load always is less in the case when the inertia of the string is included.

An easy experiment that compares the approximate and exact expressions for the aforementioned transverse frequency ratio to its experimentally determined values for identical loaded and unloaded rubber strings is described in Sec. III. Three kinds of rubber cords subjected to stretches ranging up to nearly 400% elongation were studied for a wide range of centrally attached loads, the period of vibration being measured with a novel laser beam device. The experimental results, presented in Sec. IV, show remarkably good agreement with the theoretical predictions derived in Sec. II. We find no significant variation in the data among the materials used nor for the full range of stretches studied. Therefore, our experiment, extending over a wide range of loads, confirms that the ratio of the fundamental transverse vibrational frequencies of identical loaded and unloaded rubber strings that may be subjected to finite stretch is a constant that depends only upon the ratio of their masses.

II. TRANSVERSE VIBRATION OF LOADED AND UNLOADED STRINGS REVISITED

We consider an elastic, perfectly flexible string, wire, or fiber of undeformed length l_0 and total mass m stretched by a force $T(\lambda)$ to length $l = \lambda l_0$ and clamped in rigid supports at both ends. We shall neglect gravity, momentarily ignore the inertia of the string itself, and focus our attention on a centrally attached load of mass M that is given a small displacement normal to the string and released to perform small oscillations of circular frequency ω and amplitude $A \leqslant l$. The tension is assumed constant at all times t during the motion $Y(M, t)$ of M, which is determined by the differential equation

$$\frac{d^2Y}{dt^2} + \omega^2 Y = 0 \qquad (1)$$

with

$$\omega = 2\sqrt{\frac{T}{Ml}} = 2\sqrt{\frac{T/\lambda}{Ml_0}} \tag{2}$$

The solution of (1) yields the small-amplitude, simple harmonic motion of M:

$$Y(M, t) = A\cos(\omega t - \phi) \tag{3}$$

The amplitude A and phase angle ϕ are constants determined by specification of the initial data as usual.[2]

If the load is attached to the string at distance $a \equiv \alpha l$ from one end, the circular frequency for the small amplitude motion (3) is given by

$$\omega = \sqrt{\frac{T/\lambda}{Ml_0\alpha(1-\alpha)}} \tag{4}$$

This reduces to (2) when $\alpha = \frac{1}{2}$. The derivation of (4) provides an easy exercise for the student.

When the load is removed, but the aforementioned circumstances are otherwise the same, the equation for the motion $y(x, t)$ of a particle of the string distant x from one end is given by

$$\frac{\partial^2 y}{\partial t^2} = c^2\frac{\partial^2 y}{\partial x^2} \tag{5}$$

with $c = \sqrt{(T/\rho)}$, where $\rho \equiv m/l$ denotes the mass per unit length of the stretched string.[1] In this case, the general solution of (5) that meets the fixed end conditions $y(0, t) = 0$, $y(l, t) = 0$ for all times t delivers the motion

$$y(x, t) = \sum_{n=1}^{\infty} A_n\cos(\Omega_n t - \phi_n)\sin(n\pi x/l), \tag{6}$$

wherein the normal-mode circular frequencies are defined by $\Omega_n = n\pi c/l$, $n = 1, 2, 3, \ldots$, and the constants A_n and ϕ_n are determined from assigned initial conditions.[1] With the definition of c in (5), the circular frequency $\Omega \equiv \Omega_1$ of the fundamental mode is given by

$$\Omega = \frac{\pi}{l}\sqrt{\frac{T}{\rho}} = \pi\sqrt{\frac{T/\lambda_0}{ml_0}} \tag{7}$$

The relations (2) and (7) show that in either case the transverse vibrational frequency depends on the length of the string, the amount of stretch and the elastic response of the material. In particular, a rubber cord having an undeformed cross sectional area A_0 and elastic modulus E may be characterized by the constitutive equation

$$T(\lambda) = \frac{1}{3}A_0E(\lambda - \lambda^{-2}) \tag{8}$$

Of course, in this case the stretch λ may by fairly large.[2] On the other hand, for a linearly elastic, metal wire characterized by

$$T(\lambda) = A_0E(\lambda - 1) \equiv A_0E\,\epsilon, \tag{9}$$

the strain ϵ is infinitesimal so that terms of the order ϵ^2 are negligible. Therefore, in (2) and (7) the length $l = \lambda l_0$ and the mass density $\rho = \lambda \rho_0$ in the deformed state may be confounded with their values l_0, ρ_0 in the natural state; that is, for a metal wire, $T(\lambda)/\lambda = T(\lambda) - O(\epsilon^2)$, very nearly. It is clear that the exact expressions derived above must be employed when the strain if finite; consequently, in both the loaded and unloaded cases, the transverse frequency for these materials certainly will differ significantly. We shall see that the rubber cord exhibits especially interesting behavior.

Substitution of (8) into (7) yields

$$\Omega = \Omega_0\sqrt{(1-\lambda^{-3})} \text{ with } \Omega_0 \equiv \pi\sqrt{(A_0E/3ml_0)}, \tag{10}$$

whereas use of (9) gives

$$\Omega = \Omega_0\sqrt{(3\epsilon)} \tag{11}$$

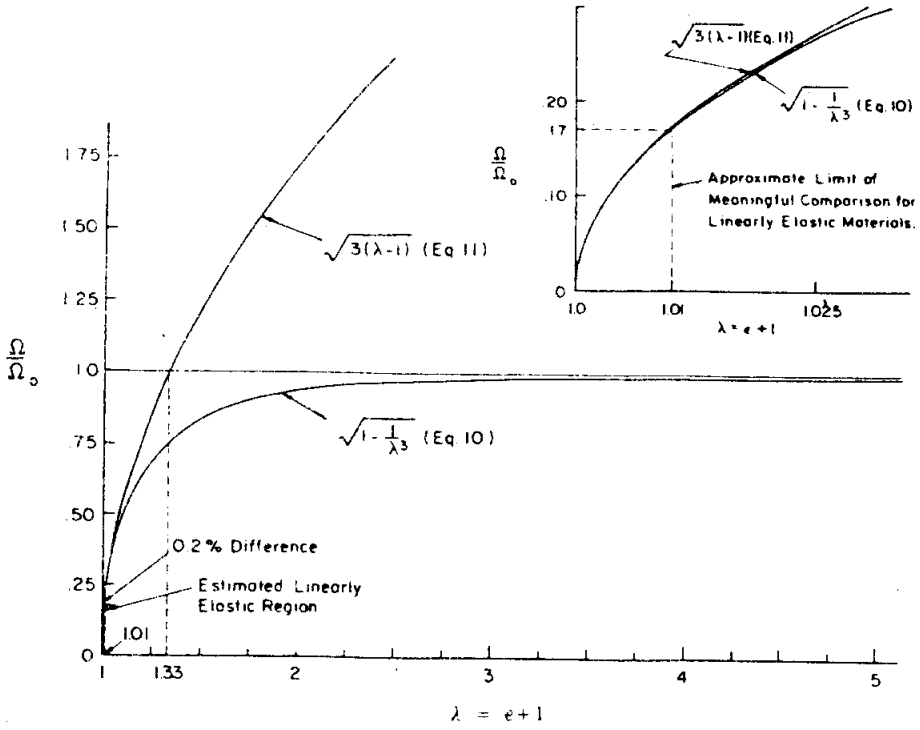

Fig. 1. Normalized transverse vibrational frequency of a linearly elastic string and a rubberlike, nonlinearly elastic cord as a function of the stretch. Upper right-hand corner: Magnification of the linearly elastic region for which (11) holds.

for the unloaded case. Similar equations can be written for the loaded case (2). It is easy to see that (10) reduces to (11) when the deformation of the rubber cord is infinitesimal; so, according to (11), for sufficiently small deformation, the squared frequency increases linearly with the stretch. But (10) reveals that as the stretch of the rubber cord increases, the transverse frequency approaches a constant value. This behavior is illustrated in Fig. 1. The graph of (11), though drawn for comparison with the expression (10) valid for large deformations of certain rubberlike materials, actually applies only over a very small range of deformation, which is shown with slight exaggeration in the upper right-hand corner of Fig. 1. The difference between the actual values on these curves at 1% strain is roughly 0.2%.

Thus we reach the interesting result derived by Beatty and Chow[3] that when a rubber band characterized by (8) is stretched sufficiently between the fingers of both hands and plucked, the pitch will vary only slightly as the tension is increased. In fact, the first experimental investigations of this phenomenon were reported independently at the turn of this century by von Lang[4] and Baker[5], although neither author was able to relate his data to a theoretical model as we have done here. Of course, the foregoing analytical prediction that so far as variation in frequency is concerned the sound power radiated by a rubber string is bounded is predicated upon a specific and simple constitutive model for rubber, commonly called the neo-Hookean model; other acceptable models of rubber elasticity[2], of which the neo-Hookean theory is a special case, may yield significantly different results, as shown by Beatty and Chow[3]. However, we wish to focus on another issue.

Let us observe that regardless of the length, the stretch or the elastic stiffness of the string the ratio R of the transverse vibrational frequencies (2) and (7) of identical loaded and unloaded strings is a constant that depends solely upon the ratio of the string mass to the load mass:

$$R = \omega/\Omega = (2/\pi)\sqrt{(m/M)}. \tag{12}$$

Since, in effect, we have assumed that the mass of the string is small compared with that of the load, it is evident from (12) that the vibrational frequency of the load always is less than the fundamental frequency of the string. Let us now review the more difficult case when the inertia of the string is included and all other assumptions are the same as before.

The load is identified as a particle of mass M attached to the string distant a from one end so that its motion $Y(M, t)$ coincides with the motion $y_r(a, t)$ of the point at $x = a$ on the parts $r = 1, 2$ of the cord. Then, for continuity at $x = a$, for all times t

$$Y(M, t) = y_1(a, t) = y_2(a, t). \tag{13}$$

the motion $y_r(x, t)$ of each part of the string is determined by (5):

$$\frac{\partial^2 y_1}{\partial t^2} = c^2 \frac{\partial^2 y_1}{\partial x^2}$$

$$\text{on } 0 \leqslant x \leqslant a \text{ with } y_1(0, t) = 0, \tag{14}$$

$$\frac{\partial^2 y_2}{\partial t^2} = c^2 \frac{\partial^2 y_2}{\partial x^2}$$

on $a \leqslant x \leqslant l$ with $y_2(l, t) = 0$ (15)

Further, since the string tension has been approximated for all times by its uniform equilibrium value, the tension must be the same throughout both parts of the string during the small amplitude oscillation of the system. It therefore, follows that the motion of M is governed by the differential equation

$$\frac{d^2 Y}{dt^2} = \frac{T}{M}\left(\frac{\partial y_2}{\partial x} - \frac{\partial y_1}{\partial x}\right)\Big|_{x = a}$$

We seek solutions of the form $y_r(x, t) = A_r(x)e^{i\omega t}$, which will satisfy (14) and (15), and thus obtain

$$y_1(x, t) = Ce^{i\omega t}\sin\mu x \text{ for } x\epsilon\ [0, a], \tag{17a}$$

$$y_2(x, t) = De^{i\omega t}\sin\mu(l - x) \text{ for } x\epsilon\ [a, l] \tag{17b}$$

Here C and D are certain constants and $\mu \equiv \omega/c$. Equation (13) requires

$$Y(M, t) = Ce^{i\omega t}\sin\mu a = De^{i\omega t}\sin\mu b,$$

Where $b \equiv l - a$. Therefore, the motion of M is described by

$$Y(M, t) = Ae^{i\omega t} \tag{18}$$

with $A = C\sin\mu a = D\sin\mu b$. Consequently, if the point $x = a$ is not a nodal point for which $Y(M, t) = 0$, that is, $A \neq 0$, (17) delivers

$$y_1(x, t) = Y(M, t)\frac{\sin\mu x}{\sin\mu a} \text{ for } x\epsilon\ [0, a], \tag{19a}$$

$$y_2(x, t) = Y(M, t)\frac{\sin\mu(l - x)}{\sin\mu b} \text{ for } x\epsilon\ [a, l]. \tag{19b}$$

However, if the point $x = a$ is nodal, (17) must satisfy

$y_1(a, t) = y_2(a, t) = 0$. Then M remains at rest as the two parts of the cord oscillate with frequency determined by $\mu a = s\pi$, and b is a suitable multiple of a such that $\mu b = q\pi$, where $s, q = 1, 2, 3, \ldots$ Otherwise, substitution of (19) into (16) yields (1) with

$$\omega^2 = \mu^2 c^2 = (T\mu/M)(\cot\mu a + \cot\mu b);$$

that is, with $c^2 = T/\rho$ and $m = \rho l$,

$$\mu l = \gamma(\cot\mu a + \cot\mu b), \tag{20}$$

where $\gamma \equiv m/M$.

This transcendental equation determines $\mu = \omega/c$ when the other parameters are assigned. In particular, when $a = b = 1/2$, we obtain the simpler formulas

$$\theta\tan\theta = \gamma \text{ with } \theta \equiv \mu l/2 = \omega\pi/2\Omega, \tag{21}$$

wherein we recall (7) and the previous relation for c in (5). Equation (21) determines $\theta = \theta(\gamma)$ for all values of the mass ratio γ. This result demonstrates that when the inertia of the string

is taken into account, the ratio R of the fundamental transverse vibrational frequencies of a loaded and an otherwise identical unloaded string is a constant that depends solely on the ratio of their masses, that is,

$$R \equiv \omega/\Omega = (2/\pi)\theta(\gamma) \tag{22}$$

is independent of the amount of stretch and the nature of the material.

When only terms of second order in θ are retained in the series expansion of (21), we have $\theta(\gamma) = \sqrt{\gamma}$. Hence, if γ is considerably smaller than one, use of this approximation in (22) yields our earlier result (12) for which case the mass of the string is negligible compared to that of the load. To obtain the lowest-order correction that accounts for the inertia of the string, Terms of the fourth order in θ are retained in (21) ; we find

$$\theta(\gamma) = (1 - \gamma/6)\sqrt{\gamma} \tag{23}$$

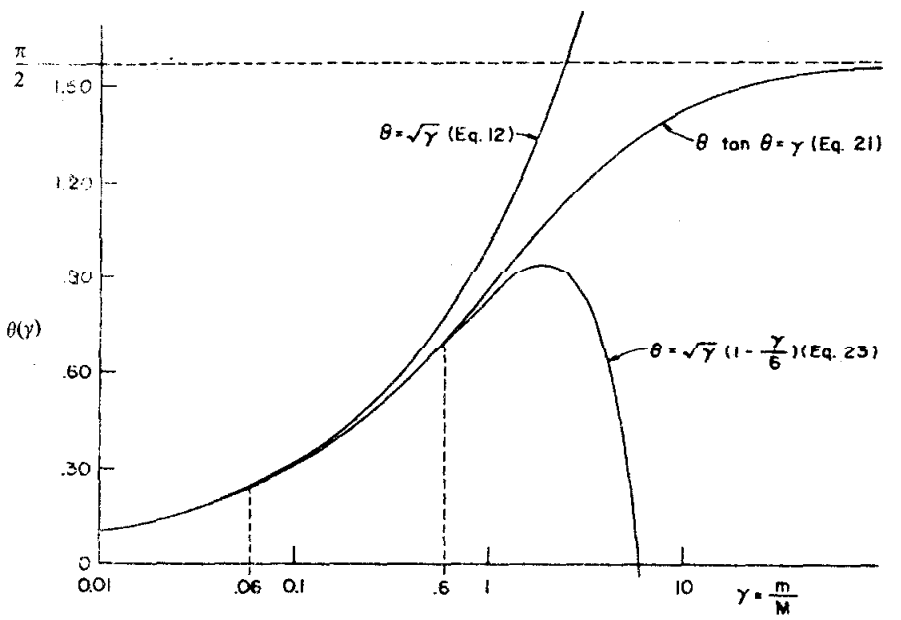

Fig. 2. Comparison of first and second order approximate solutions with the act solution for the transverse oscillatics of a centrally loaded string in the funds mental mode (semilog graph).

Here γ must be small enough that terms of second order in γ are negligible. For the lowest mode, these approximate solutions are compared graphically with the exact solution (21) in Fig. 2 for $\theta \epsilon$ (0, n/2). The simple solution (12) approximates the exact curve (21) to only 1% error at $\gamma = 0.06$, so (12) is an accurate estimate for heavily loaded strings. The second-order solution (23) extends this range to alomost $\gamma = 0.60$ where the simple solution errs by nearly 10%. In fact, we see that (23) approximates (21) nicely for, $\gamma \leqslant 1$ at which value the error is roughly 3%. Nevertheless, the experiments to be described later on for lightly to heavily loaded rubber strings will extend well beyond the range of applicability of even the second-order solution.

More generally, the positive solutions θ_n, n = 0.12, ... of (21) and the aforementioned nodal solutions $\theta = s\pi$, s = 1, 2, 3, . . . (which are independent of M) also may be graphically

illustrated. The θ_n are the points of intersection of the graphs of the trigonometric function $z = \tan\theta$ and the rectangular hyperbola $z = \gamma/\theta$ shown in Fig. 3. The unique solution $\theta = \theta_0 \in (0, \pi/2)$ is the exact value for the dominant mode. Since all higher modes tend to and are preceded by nodal values, we may write for the nth root of (21)

$$\theta_n = \theta_n' + \delta_n = n\pi(1 + \delta_n/n\pi) \quad \text{for} \quad n = 1, 2, 3, \ldots$$

To the first order in δ_n, (21) yields $\delta_n = \gamma/n\pi$, hence, the roots of (21) are approximated by

$$\theta_n = n\pi(1 + \gamma/n^2\pi^2) \quad \text{for} \quad n = 1, 2, 3, \ldots \tag{24}$$

when γ is sufficiently small. Of course, the general relation (21) is valid for all γ and always may be used to find the effect on the frequency of the various component vibrations due to even a small mass M attached to a considerably more massive string.

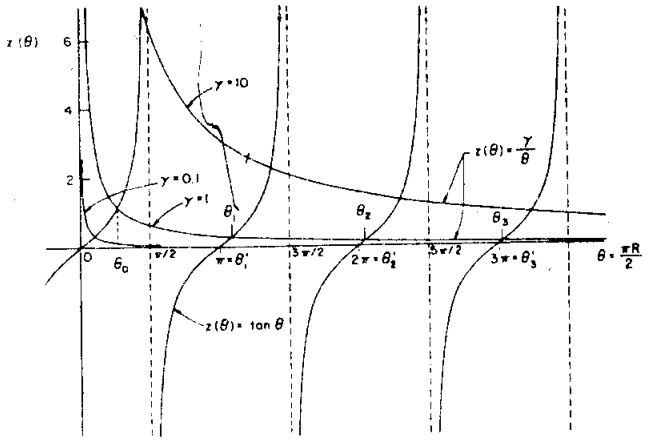

Fig. 3. Graphical illustration of several higher-mode solutions and neighboring nodal solutions for selected values of γ, θ_0 indicates a typical dominant fundamental mode of principal interest.

Finally, let us write ω_0 for the circular frequency (2) of the load when the inertia of the string is neglected. Then use of (7) in (22) shows that $\omega = \omega_0\gamma^{-\frac{1}{2}}\theta(\gamma)$, and application of the first-order correction for the inertia of the string in (23) reveals that

$$\omega = \omega_0(1 - \gamma/6) < \omega_0 \tag{25}$$

Indeed, the graph in Fig. 2 shows clearly that the exact solution (21) for $\theta(\gamma)$ always lies below the simple solution (12). Thus the circular frequency ω of the load always will be less in the case when the inertia of the string is taken into account. Equation (25) also shows that, to the first order in γ, the error in frequency due to neglecting the mass of the string itself is

$$(\omega_0 - \omega)/\omega = \gamma/6 \tag{26}$$

Here we are able to see clearly that this error will be small only when γ is small, i.e., only when $M >> m$

III. EXPERIMENTAL APPARATUS AND PROCEDURE

A simple laboratory experiment that serves to reinforce these rudimentary physical results has been developed. This experiment compares the simple and exact predictions of R, (12), (23), and (21), respectively, to an experimentally determined R. The apparatus, which was developed by Beatty and Chow[3] to measure the transverse vibrational frequency of rubber strings, is shown in Fig. 4 ; it consists of 3 bridge carriage to support the cord, a laser light source and photoelectric cell receiver whose output is fed into an electronic digital counter that records the average over several cycles of either the frequency or the period of the oscillation. However, the period could be measured more accurately. The laser beam provided a narrow, concentrated light beam that was focused normally to the midpoint of the string and directly in front of the photoelectric cell aperture. The string was plucked at its midpoint, and its transverse motion in the plane normal to the beam interrrupted the laser twice in each cycle. Therefore, the counter recorded half the actual period of the vibration.

Gum rubber, neoprene, and buna-N rubber materials were used. All of the strings were fabricated from standard 40 durometer rubber *"O"* -ring cord of nominal diameters 2.362 mm. (0.093 in.) for the gum rubber and 2.616 mm. (0.103 in.) for the others. The manufacturer's standard dimensional tolerance was specified as ± 0.127 mm. (±0.005 in.) for all three varieties. Three samples of the buna-N and one sample of each of the other materials were tested. The samples were cut in nominal lengths of 50.8 cm. (20 in.) from rolls of stock and weighed in order to determine their natural state mass density ρ_0. In order to test the same set of mass ratios γ for each string, using an assigned set of loads M, each string's test segment, that portion between the bridge support, was to be of the same mass. A 10-in. segment of buna-N rubber cord was arbitrarily selected as the reference mass. Then, the gum rubber sample, which was of lower density, and the neoprene sample, which was of higher density, were marked off in the lengths l_0 shown in Table I. We note that for two measurements of the group rubber sample, the test segment l_0 was reduced to 10 in. so that its maximum stretched length would not exceed the expanded bridge length, thus reducing the values of γ. Proper allowances were made in calculations.

The loads consisted of six small, axially symmetrical metal weights having an axial hole through which the string could be threaded. The hole was about half of the string's natural state diameter d_0, in order that, after threading the string through the hole while at high stretch, releasing it to a lower stretch or to its natural state had the effect of clamping the load tightly in place at the midpoint of the test segment. The masses of the loads, ranging from 0.38 to 13.81 g, were selected so as to provide a wide range of ratios γ. We also found that the average values of d_0 determined for several samples of the stock material did fall within the aforementioned tolerances ; these are given in Table I.

Owing to relaxation effects the strings exhibited continual, though small, variation

in tension. With the counter averaging the period over 10 cycles; this led to small fluctations of the order $\pm 10^{-3} - \pm 10^{-4}$ sec in the period reading. In an effort to control variable tension effects, the periods for ω and Ω were read in quick succession and at the smallest possible amplitude of oscillation. The experiment proceeded as described below.

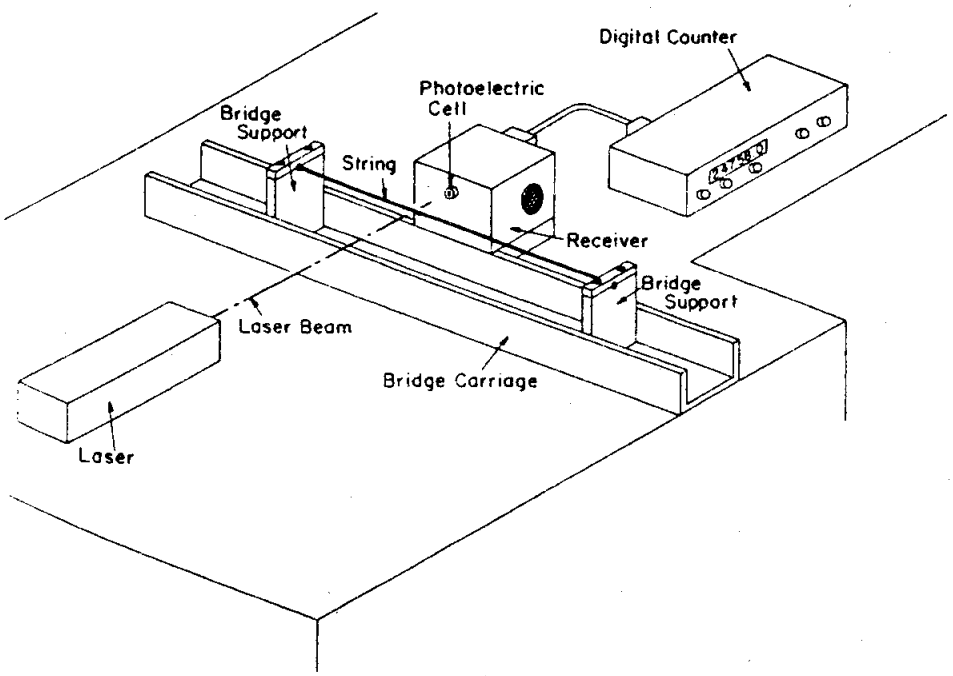

Fig. 4. Schematic of the experimental apparatus for measurement of transverse frequency of vibration of a rubber string.

Table I. Physical properties of the strings.

Material	d_0(mm)	ρ_0(kg/m)	l_0(cm., in.)	m (kg) (test segment)
Buna-*N*	2.602	5.689×10^{-3}	25.4, 10.0	1.445×10^{-3}
Natural gum	2.390	4.764×10^{-3}	30.3, 11.9	1.445×10^{-3}
neoprene	2.556	6.693×10^{-3}	21.6, 8.50	1.445×10^{-3}

The ends of the test segment were clamped to movable bridge supports separated initially be distance l_0. The supports were then further separated symmetrically in the carriage to increase the stretch λ, which was measured to with in ±0.5 mm. (± 1/64 in.) by a calibrated tape fastened to the bridge carriage. Six values of stretch covering a wide range of elongation were tested in increasing order. The unloaded string was taken to the lowest

state of stretch plucked at its midpoint, and the unloaded period measured. Then, the smallest load was quickly added at the center, the string plucked again, and the loaded period measured. After a brief pause, the loaded period was again measured, the load quickly removed, and the unloaded period measured. These four measurements were used to compute R for the given γ, λ and modulus E (i.e., material). The load was then increased, while holding λ constant, and the process repeated. When all six loads had been tested, the stretch was increased and the entire procedure repeated. In this manner the frequency ratio R was determined using the same wide variety of γ's and λ's for each of the three kinds of material studied.

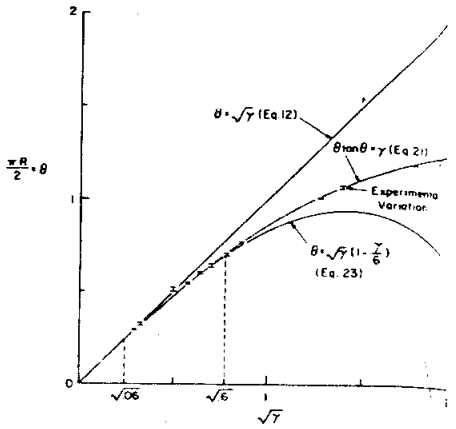

Fig. 5. Compasion of experimental and theoretical results for θ (γ) determined for a neoprene rubber cord when the stretch is varied at each value of γ.

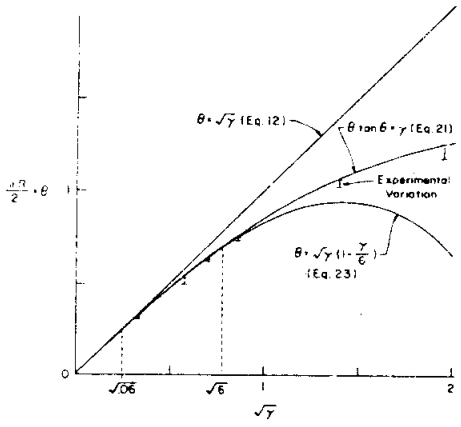

Fig. 6. Comparison of experimental and theoretical results for θ (γ) determined for a gum rubber string when the stretch is varied at each value of γ.

IV. SUMMARY AND DISCUSSION OF THE EXPERIMENTAL RESULTS

The test results are summarized in Figs. 5-8. The data obtained for the single neoprene and gum rubber samples are plotted in Figs. 5 and 6, respectively. The I symbols shown at various fixed values of γ denote the range of variation in the experimentally determined values of θ as the stretch was increased over its range from 1.20 to 3.70 in increments of 0.5 Similarly, the data for the values of θ averaged from the three tests on buna-N rubber cord, for the same stretches, is presented in Fig. 7. The graph in Fig 8 shows the variation in the experimental values of θ when, for each stretch in the above range, the values of θ for all the materials are averaged together. Thus congruent with the theoretical expression derived here, the data confirms that the frequency ratio is independent of the amount of stretch and the nature of the material. Indeed, the results of the experiment correlate very well with the prediction of the exact relation (21). It is seen in Figs. 5-8 that the experimental values of R fall on or quite near the graph of the theoretical prediction over the whole range of γ's and λ's tested and manifest no significant variation among the several materials used.

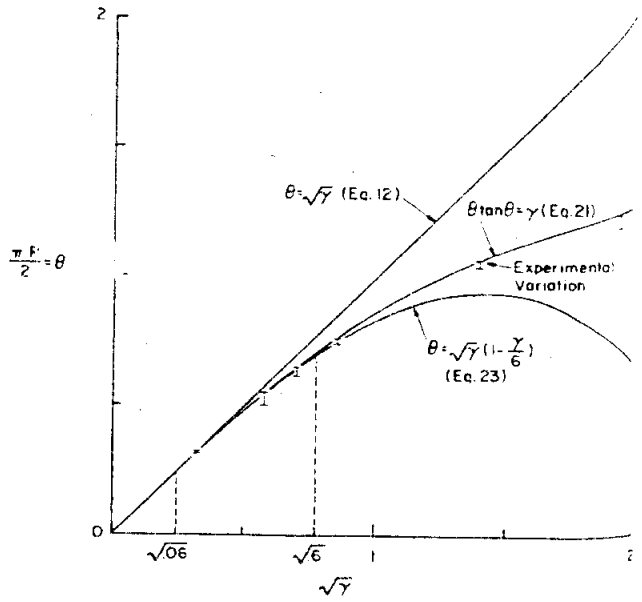

Fig. 7. Comparison of theoretical results with experimental values of θ averaged from three tests on Buna-N rubber cord as the stretch was varied over the same range at each value of γ.

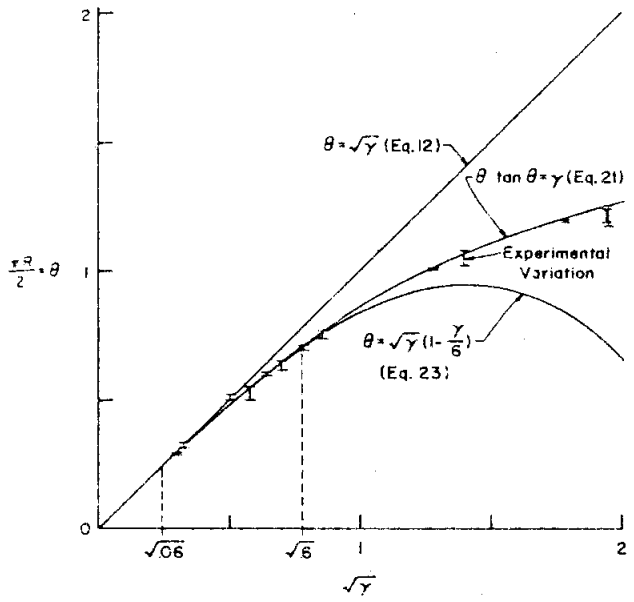

Fig. 8. Comparison of theoretical results with experimental values of θ for all materials averaged together over the same range of stretch at each value of γ.

We observe some increase in the variation of R at the highest values of γ, at least in part due to experimental difficulties associated with the use of the small masses needed to produce large γ's. Irregularities in the small masses introduced slight rotational effects that tended to damp vibrations to a greater extent than for larger masses, making readings more erratic as well as decreasing the number of measurable cycles. We note, however, that irregularities in the shapes of the loads had some effect at all values of γ and that this effect has been neglected here.

For the lowest value of stretch ($\lambda = 1.20$), at which tension was least, vibrations were difficult to sustain; in fact, the buna-N strings would not vibrate in any measurable fashion at the smallest γ for this value of stretch. Deviations from the theory consistently decreased as the stretch was increased for the buna-N data set. The decrease was sharpest when the stretch was increased from 1.20 to 1.70 and slower thereafter. This behavior is consistent with the theoretical assumption of constant tension. In the gum rubber tests, which show exceptionally good agreement with (21), this trend occurred to a lesser extent; in the neoprene data it was not apparent.

For the gum rubber tests we recall that the string was shortened to accommodate two measurements at high stretch. We note that the data continued to follow the theory well, except for the two measurements at $\sqrt{\gamma} = 0.50$, shown in Fig. 6 These measurements differed fairly widely probably due to some random effect involving the mass used for this γ.

For the buna-N and neoprene strings there existed some tendancy for the experimental R values to fall short of the theoretical values. This effect was smaller in the gum rubber tests, but in all tests was more pronounced at larger values of γ. The buna-N data indicates that this effect is largely the result of the aforementioned tension effects at low stretch. In the order data no cause seems evident. Of course, unknown effects due to damping are also present in all cases.

Excessive gravitational deflection prohibited tests in the region of very small γ values where the first approximation is valid to less than 1% error at $\gamma = 0.06$, but we note from Figs. 5-8 that the data fits the first approximation accurately at small values of $\gamma < 0.10$. On the other hand, the experiment shows excellent agreement with the second-order approximation over its full range of applicability and somewhat beyond the point of 1% error at $\gamma = 0.6$, roughly up to $\gamma = 0.75$, as shown in Figs. 5-8.

In sum, the results confirm that our theoretical equation (22), based on the constant tension assumption for small amplitude oscillations of identical loaded and unloaded rubber strings, is quite accurate for all materials tested and for all values of the stretch. Thus this experiment, extending over a wide range of mass ratios, confirms that the ratio of the fundamental transverse vibrational frequencies of identical loaded and unloaded rubber strings that can be subjected to finite stretch is a constant that depends solely on the ratio of their masses. It is our view that this example, which is a fragment extracted from a deeper research program in finite elasticity, constitutes an excellent laboratory exercise for students.

ACKNOWLEDGMENT

This work was done in the course of a research study that was partially supported by the U.S. Department of Transportation and the U.S. National Science Foundation.

---

[1]Lord Rayleigh (John W. Strutt), *Theory of Sound* (Macmillan, London, 1944).

[2]L.R.G. Treloar, *The Physics of Rubber Elasticity,* 3rd ed. (Clarendon, Oxford, 1958).

[3]M.F. Beatty and A.C. Chow, *J. Elasticity* (to be published).

[4]V. von Lang, Am. *Phys. Chem.* 68, 335-342 (1899).

[5]T.J. Baker, *Philos. Mag.* 49, 347-351 (1900).

หนังสืออ้างอิง

Meyer, Stuart L., *Data Analysis for Scientists and Engineers.* 1st ed. New York : Wiley, 1975.

Am. J. Phys. 50(1) Jan. 1982. p. 38-42.

Am. J. Phys. 50(2) Feb. 1982. p. 113-119.

Electron Diffraction

หนังสืออ้างอิงสำหรับเขียนทฤษฎีและเพื่อการค้นคว้าทั่วไป

Anderson, E.E., *Modern Physics and Quantum Mechanics,* 1st ed., Philadelphia : Saunders, 1971

Blatts, F.J. *Principles of Physics,* 1st ed., Boston : Allyn and Bacon, Inc., 1983.

Borowitz, S. and Bornstein, L.A. *A Contemporary View of Elementary Physics,* 1st ed. New York : McGraw-Hill, 1968

Crawford, Jr., F.S., *Waves,* 1st ed. New York : McGraw-Hill, 1968.

Einsberg, R.M. and Lerner, L.S., *Physics,* 1st ed., New York : McGraw-Hill, 1982.

Gartenhaus, S., *Physics* 1st ed., New York : Holt, Rinehart and Winston, Inc., 1975.

Giancoli, D.C., *General Physics,* 1st ed., New Jersey : Prentice-Hall, Inc., 1984.

Harnwell, G.P. and Livingood, J.J., *Experimental Atomic Physics,* 1st ed., New York : McGraw-Hill, 1933.

Marion, J.B., and Hornyak, W.F., *Principles of Physics,* 1st ed. Philadelphia : Saunders, 1984.

Sears and Others, *College Physics,* 5th ed., Mass : Addison - Wesley, 1980.

Sutton, R.M., *Demonstration Experiments in Physics,* 1st ed., New York : McGraw-Hill, 1938.

White, H.E., *Modern College Physics,* 6th ed., New York : D. Van Nostrand, 1966.